Baghdad Science Journal

Volume 22 | Issue 6 Article 16

6-20-2025

Influence Percentage of Additive Materials on the Structural and Physical Characteristics of Nickel Metal Using Thermal Spraying by Flame

Mohammed M. Hameed
Ministry of Higher Education and Scientific Research, mohammedaz365@gmail.com

Salih Y. Darweesh
Physics Department, College of Science, Tikrit University, Tikrit, Iraq, salih.younis@tu.edu.iq

Amer SH. Mahmood
Physics Department, College of Education for Pure Sciences, University of Tikrit, Tikrit, Iraq, amer.shaker@tu.edu.iq

How to Cite this Article

Hameed, Mohammed M.; Darweesh, Salih Y.; and Mahmood, Amer SH. (2025) "Influence Percentage of Additive Materials on the Structural and Physical Characteristics of Nickel Metal Using Thermal Spraying by Flame," *Baghdad Science Journal*: Vol. 22: Iss. 6, Article 16.
DOI: https://doi.org/10.21123/2411-7986.4966

BAGHDAD SCIENCE JOURNAL 2025;22(6):1919–1929

RESEARCH ARTICLE

Influence Percentage of Additive Materials on the Structural and Physical Characteristics of Nickel Metal Using Thermal Spraying by Flame

Mohammed M. Hameed [1,*], **Salih Y. Darweesh** [2], **Amer SH. Mahmood** [3]

[1] Ministry of Higher Education and Scientific Research
[2] Physics Department, College of Science, Tikrit University, Tikrit, Iraq
[3] Physics Department, College of Education for Pure Sciences, University of Tikrit, Tikrit, Iraq

ABSTRACT

The method of thermal spraying with flame, which was used to conduct a coating consisting of a nickel base and additions of three groups—(C=Ni-WC-B_4C), (B=Ni-B_4C), and (A=Ni-WC)—and with different reinforcement ratios from these groups, forms the basis of cermet coating. The bases for thermal spraying were made by roughing up and cutting out-of-service turbine blades that were 1 cm square in shape. The spray angle 90°, spray distance of 15 cm, thermal sintering temperature of 1050°C, and mixing ratio of type (C=50%Ni-25%WC-25%B_4C) of the three mixes were at their ideal standard conditions. The results of the scanning electron microscope showed nearly good mechanical homogeneity and crosslinking at the same percentage above, especially after the thermal sintering process. It was discovered that the hardness is (240 Hv), the adhesion strength is (39 MPa), and the best coating thickness at each of the hardness and adhesion strength is (1.5 mm). The (C) mixture, which had superior structural, physical, and mechanical capabilities compared to the (B) and (A) combinations, was also reported to have produced the best outcomes.

Keywords: Boron carbide, Cermet coating, Coating thickness, Scanning electron microscope, Thermal spraying

Introduction

The phrase “thermal spraying” refers to a group of procedures that include depositing metallic or non-metallic materials on substrates that have been prepared in preparation for coating while they are still molten or semi-molten. Typically, the coating ingredients come in the form of metal rods or wires or powder.[1] Depending on the heat source used to melt the paint, thermal spraying processes can be divided into two categories: chemical and electrical. Flame spray, high velocity oxygen fuel spray (HVOF), and explosive spray are examples of chemical kinds (Detonation spray). The sorts of electric ones are as follows: Electric Arc Spray and Plasma Spray.[2] With the introduction of the oxyacetylene torch (Oxy-acetylene Torch) between the years (1890–1910), the thermal spraying method was discovered.[3] Following that, these technologies continued to be developed and updated. Since it used the oxy-acetylene flame and the electric arc as a source of heat between the years 1921 and 1909), the Swedish engineer (Schoop) was able to develop twelve techniques for thermal spraying. However, it was only capable of spraying metallic and ceramic materials with a low melting temperature, and only experimentally.[4] The coating ingredients are heated by the combustion of gases, such as flame spraying or electric arcs, or by an electric arc that warms and ionizes a stream of gases, as in Plasma Spray, as the coating materials are typically in their solid states.[4] The coating process can be summed up as follows: heating the material to be coated, melting it, atomizing it, speeding it up by compressing gases, and finally transferring it to

Received 5 March 2023; revised 16 April 2024; accepted 18 April 2024.
Available online 20 June 2025

* Corresponding author.
E-mail addresses: mohammedaz365@gmail.com (M. M. Hameed), Salih.younis@tu.edu.iq (S. Y. Darweesh), amer.shaker@tu.edu.iq (A. SH. Mahmood).

https://doi.org/10.21123/2411-7986.4966

the surface of the base (Substrate) by generating a precise stream of droplets and by the action of the gas push. Drops flatten and adhere to the base as they come in contact with it, generating strips that are joined to the base and to one another to produce a lamellar covering.[5] One of the crucial methods for producing protective coatings (Protection Coating) is thermal spraying technology.[6] These coatings are used for thermal insulation, protection against wear and oxidation, chemical and mechanical corrosion, rebuilding worn parts to their original dimensions, and protection against wear and oxidation. This method can be applied to coating metallic materials and their alloys, ceramic and polymeric materials, refractory metals (such as tungsten and molybdenum), even materials with super conductivity, and on a variety of substrates, starting with substrates with a low melting temperature (such as plastic) and ending with substrates with a high melting temperature (such as ceramics and refractory metals).[7] The use of thermal spraying techniques is widespread, for example in optical fields or electrical applications.[8,9] The matrix, the foundation material, is formed using thermal spraying technology when creating composite materials.[10] The study aims to improve the physical properties of the materials used in the coating using thermal spraying by flame technique.

Materials and methods

The initial support material, tungsten carbide, with a granular size of 75 μm and made by (Metco102) with a purity of (99.8%), as well as nickel metal powder with a granular size of 75 μm were both employed. The second support material was boron carbide, which had micro-grains of 90 μm in size and a purity of 99.6% and was made by Metco110. In the current study, coated samples of a system based on nickel metal were produced using three different thermal spraying by flame techniques: the first utilized different combinations of (Ni-%WC), the second used (Ni-%B_4C), and the third used (Ni-%WC-%B_4C) and in different weight ratios given in Table 1. Fig. 1 illustrates a device produced locally that mixes the powders using steel balls in a micro-mill. The device employed two acetylene oxygen bottles, with the oxygen ratio being 4 bar and the acetylene ratio being 1 bar (≈0.7 bar). After being processed for two hours in a homemade mill with steel balls, a unique powder is put inside the spray gun so that the powder can be mixed in it. The combination was then subjected to a temperature of 100°C for 30 minutes to remove the moisture from the powder. After the base mixture was sprayed with three separate mixes, the powder was deposited in the spray gun's designated powder container, which included a powder of the primer coating material with a binder of (80% Ni + 20% Al). Additionally, all combinations were taken consistently at the distance designated for coating, which is (15 cm). To increase the adhesion strength between the molten drops and the base of the coating that was used from an out-of-service turbine feather cut in a square shape with a dimension of 1 cm for each side, the powder pellet is opened and the powder starts to descend to the previously roughened base by the method of serration. According to Table 2, which displays the chemical analysis of the alloy used as a coating basis, the X-ray fluorescence analysis of the base is shown. Following the completion of the prepared models, these samples exhibit some weakness in the external coating, which urgently calls for heat treatment. This treatment was carried out for the samples through a German-made Muffle furnace for the samples for a brief time—just two hours—at a temperature of 1050°C. The next step is to carry out laboratory testing, such as physical, mechanical, and synthetic ones.

Table 1. Mixtures used in the practical part.

Type of Mixture	Concentration%
A	95%Ni + 5%WC
	90%Ni + 10%WC
	85%Ni + 15%WC
	80%Ni + 20%WC
	75%Ni + 25%WC
B	95%Ni + 5%B_4C
	90%Ni + 10% B_4C
	85%Ni + 15% B_4C
	80%Ni + 20% B_4C
	75%Ni + 25%B_4C
C	90%Ni + 5%WC + 5%B_4C
	80%Ni + 10%WC + 10%B_4C
	70%Ni + 15%WC + 15%B_4C
	60%Ni + 20%WC + 20%B_4C
	50%Ni + 25%WC + 25%B_4C

Fig. 1. Illustrate the thermal spray system.

Table 2. The chemical analysis of the alloy used as a coating basis (St.St.316L).

Elements	AISI -316L
C	pct 03.0<
Si	pct 00.1<
Mn	00 pct .2<
P	Pct 04 .0=<
S	03 pct .0=<
Cr	pct 00 .17
Mo	25 pct.2
Ni	00 pct .12
Fe	Remain

Utilized tests

Hardness test

Hardness is the ability of a material to resist persistent deformation (plastic deformation, which happens as a result of indentation, cutting, wear, and scratching), penetration, and machinability. The kind of bonding force affects how hard a material is. Among atoms or molecules, the type of surface, high temperature, and heat treatment. The Vickers micro-hardness test was performed using a French-made hardness device of the type (METKON), which includes a penetration tool that has a pointed microscopic head shaped like a diamond pyramid with a square base and levels that intersect at an angle of 136° at the top. The sample is fixed underneath this tool for the test. The samples were divided into pieces measuring 1 cm in length, 1 cm in width, and 1 cm in thickness. A force of 50 N was applied for 20 seconds. By measuring the lengths of the two diameters (d_2, d_1) and their average values (D), and then using the connection, the Vickers hardness number is determined by Eq. (1).[11]

$$\mathbf{HV} = \mathbf{1.854}\ \frac{\mathbf{P}}{\mathbf{d_{av}}} = \ \mathbf{HV} = \ \frac{\mathbf{2Psin}\frac{\mathbf{136^{\circ}}}{\mathbf{2}}}{\mathbf{d_{av}}} \qquad (1)$$

Where *HV* is Vickers hardness, *P* the applied load (N) and *dav* represent mean impact diameter.

A rough estimate of the hardness rate was obtained by measuring the hardness in several distinct places of the sample, including the center and the edges.

Adhesion force

The painted model is the primary component of the task, thus it is required to calculate the adhesion force, which is the adhesive force between the system's coating and the base, which is meant to depict an oil pipe or a turbine vane. (Time Group lnc.) When a coated and uncoated sample is taken; an adhesive is placed between the two samples and pressed using the device (Universal Testing Machine Type Hoytom)

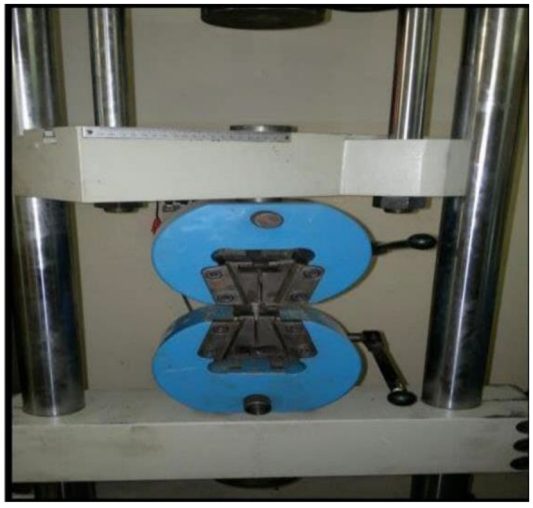

Fig. 2. Shows the adhesion force device.

for a period of 24 hours. Then, the above device is used to pull between the coated and uncoated sample, and when the two samples are uncoated, the adhesive is measured in units of (MPa). As demonstrated in Fig. 2, some devices will record the highest contact force in Pascal's.[12]

Wear test

The wear rate of coating samples made of mixed material was measured using the (Amsler) equipment. The wear tester comprises of a set gears with the an axis for attaching the paint sample and an electric motor revolving at a rotational speed of (190 rad/min). In order to gauge the degree of wear, the disk on disk approach was used. The quantity of paint loss due to sliding wear was also determined using the weight method. Before and after the wear, the sample is weighed on a sensitive scale with a sensitivity of (±0.001 g), using a type (Metll H311). The sample is positioned in the Amsler device's assigned location, in close proximity to a fixed disc of high hardness, and while being subjected to a force (100 N). The test was continued for 30 minutes, and the wear rate could be estimated by using the following equation.[13]

$$\mathbf{Wear\ Rate} = \frac{\mathbf{M1} - \mathbf{M2}}{\mathbf{D}} \qquad (2)$$

Whereas: M1 represents the sample's mass prior to investigation, M2 represents the sample's mass following examination, and, D: the route taken during the examination, D: the route taken during the examination, like in:

$$\boldsymbol{D} = \mathbf{2}\boldsymbol{r}^{-}\boldsymbol{\pi}\boldsymbol{n}^{-} \qquad (3)$$

Where: r^- is the sample's radius (20 mm), and the number of cycles is n^- (calculated from the number of cycles in the test device).

Porosity

The quantity of percentage of pores on the surface of the coating, which is directly proportional to the hardness, is one of the physical tests of great importance for measuring the number of pores present within one sample. Porosity increases with weaker hardness and vice versa. The following Eq. (4) was then applied, as the Archimedes immersion method was used (Immersion Method), where the weight of the paint was calculated, which is (W1), after which the painted model was immersed in distilled water for a period of 24 hours, and then the weight was calculated after immersion (W2). The painted model was then suspended in distilled water, and the third weight (W3) was calculated.[14]

$$\textbf{Porosity} = \left(\frac{\mathbf{W_2} - \mathbf{W_1}}{\mathbf{W_2} - \mathbf{W_3}}\right) \times 100\% \quad (4)$$

Scanning electron microscope

In order to understand the outer surface of the generated samples and how they are cohesive, the surface topography of the samples formed was investigated. Due to its many benefits, including its ability to magnify objects up to hundreds of times more than light microscopes while providing a distinct description of the external surface structure, a scanning electron microscope was employed for this task. The kind of microscope being utilized is a TESCAN with a French-made model named MIRA3.

Results and discussion

The findings from looking at a few physical characteristics of the prepared samples are summarized below. Because the results acquired before conducting the thermal sintering process were insufficient and weak, these samples were tested under the most critical standard conditions, the most critical of which was after conducting the thermal sintering process for the samples.

The effect of reinforcement materials on the coating hardness

The relationship between the reinforcement additive content and the Vickers hardness values after sintering, obtained during the sintering process is depicted in Fig. 3. for various reinforcement addition proportions. When the reinforcement material was added in different amounts, the Vickers hardness value increased. The best reinforcement ratio was achieved at the mixture (Ni-WC-B_4C) 25% by (240 Hv). As the sintering process increased the results of the Vickers hardness, it can be seen that adding the content of the reinforcement material resulted in a rise in the percentages of the Vickers hardness values, with the content of the reinforcement material obviously increasing the Vickers hardness values. The percentage of Vickers hardness values in the three mixtures increased to a specified percentage, which is the ratio (50%Ni-25%WC-25%B_4C), as a result of increasing the content of the reinforcement material. The addition of the reinforcement material B_4C results in the coating, and as a result, the expansion and multiplication of the contact surfaces. The heat treatment is the second factor that increased Vickers hardness, and this is because it increased the homogeneity and bonding of the coating layers. Heat reduces pores and their size, which increases the homogeneity of the coating components and, in turn, lowers the sublime values, increasing the hardness values.[15]

Effect of coating thickness on vickers hardness

Experimental research verified a relationship between the thickness of the cermet coating layers and the distribution of surface flaws that affect hardness after sintering. Given that the higher values of hardness was at (240 Hv) for the mixing ratios of (25%) of the mixture (C), after heating the samples to (1050°C), and after, it was determined that the optimal thickness is (1.5 mm) and it is free of surface flaws. As it reached (150 Hv) at the same ratio with this thickness, the hardness values were clearly on the decline, as illustrated in Fig. 4. The results also demonstrated that the hardness values of the ceramic coating layer decrease when it is less than or greater than (1.5 mm), and the onset of cracking and delamination is evident. The increase in thickness has a negative effect on all properties because the coating layers become more susceptible to cold as they thicken, leading to agglomerations. The thicknesses (1.5 mm) were chosen for physical measurements and when performing testing on samples since the layers are placed continuously and stresses arise inside the layers.[16]

The effect of additive materials on the coating ability to stick

The experimental results showed that the adhesion strength less valuable when the proportion of the additive materials is less, then this force gradually

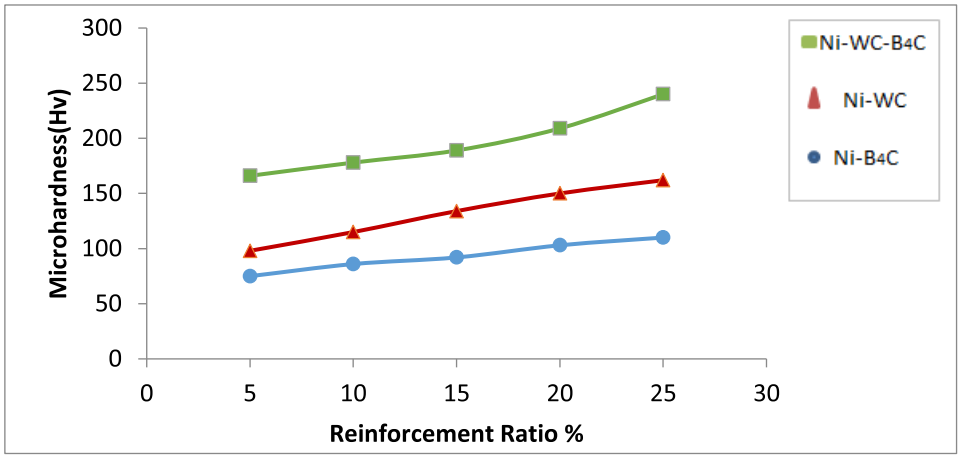

Fig. 3. The relationship between additive materials and Vickers hardness.

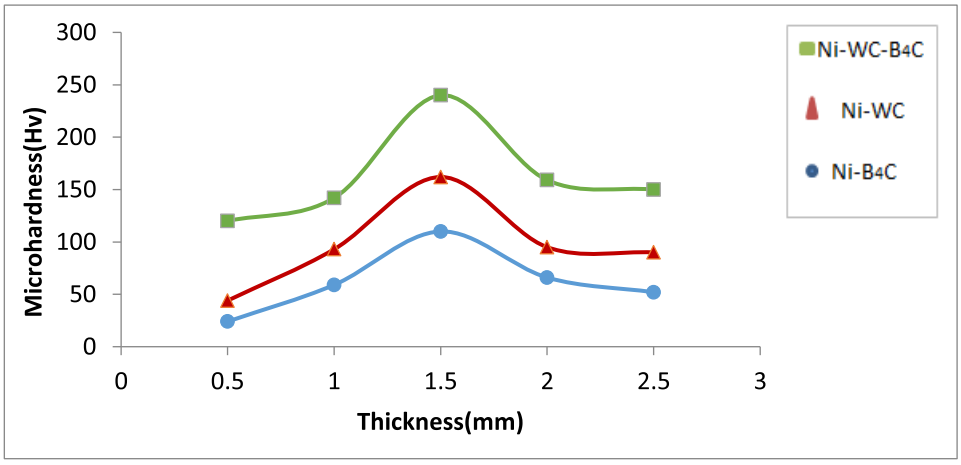

Fig. 4. The relationship between coating thickness and Vickers hardness.

increases as the proportion of the material increases until we reach the best value for the adhesion strength at the ratio (25%) of the mixture type (Ni-WC-B_4C), with a value of (39 MPa), as shown in Fig. 5. This decline happens as a result of the binding substance's efforts to weaken the adhesion between the paint layer and the base by working to establish bonding spaces between the atoms of the paint itself. As a result, both hardness and adhesion strength rise. [17]

Coating thickness's effect on adhesion strength

The results of experimental tests showed a relationship between the adhesion strength and the thickness of the cermet coating layers. As the adhesion strength was (39 MPa) for mixing ratios (25%) for all mixes steadily and after heat treatment of the samples and at 1050°C degree, it was noted that the best thickness is 1.5 mm and it is free from surface flaws, but after this thickness it lost adhesion. The hardness values clearly decreased after reaching a of 29 MPa at the same ratio, as seen in Fig. 6. The findings also demonstrated that the adhesion strength values of the ceramic coating layer decrease when it is less than or greater than 1.5 mm, and the onset of cracking and dislocation is evident. The results also showed that an increase in thickness has a negative impact on all properties because the coating layers become more prone to dislocations as they thicken. The thickness (1.5 mm) was chosen for physical measures and when testing samples because the layers continuously agglomerate and there are strains inside the layers. [18]

The effect of percentage additives materials on the rate of coating wear

Fig. 7 depicts the link between the wear rate and percentages of additive materials, which for all the developed samples reduces when the reinforcing percentage is raised. Additionally, it can be seen that the wear rate decreases when (25%) (Ni-WC-B_4C) compared with the rest of the ratios is

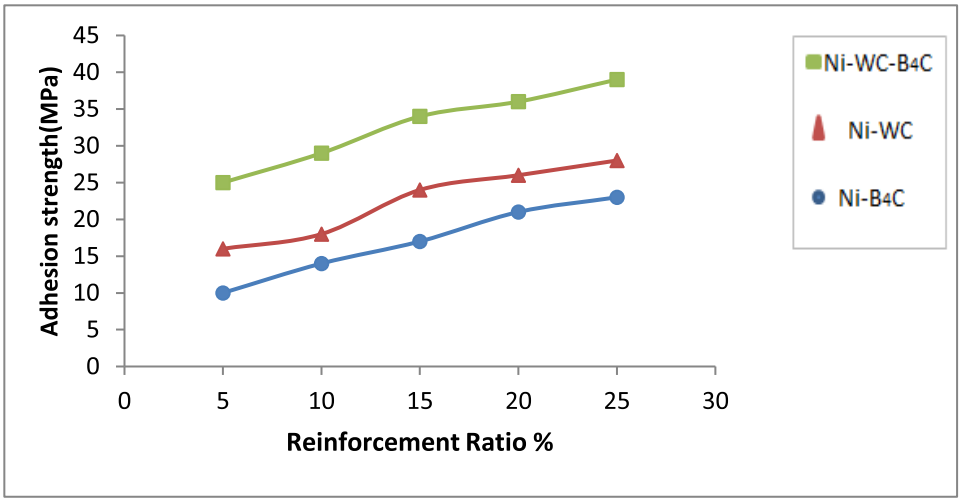

Fig. 5. The relationship between the additive materials and the adhesion strength of the coating.

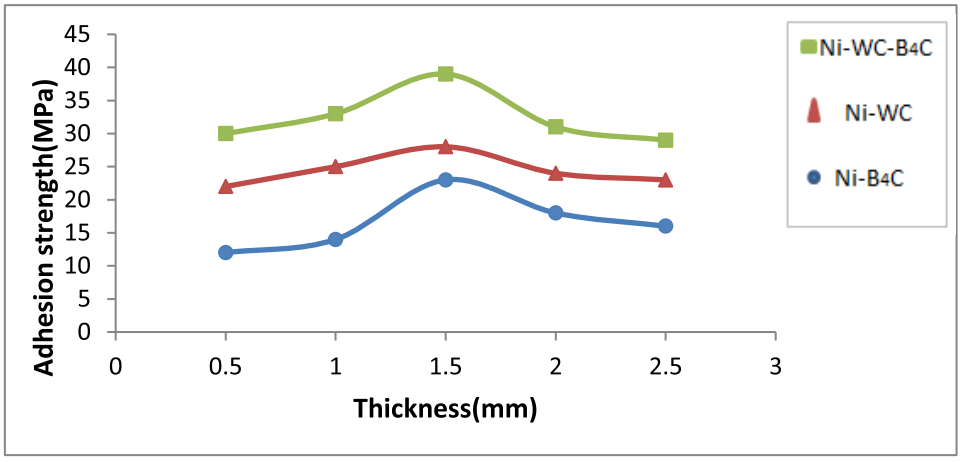

Fig. 6. Shows how coating thickness and adhesive strength are affected.

added to the mixture. As a result, the coating layers' mechanical properties improve, and their hardness increase. There is also no plastic deformation, which increases wear resistance and particle attachment to the surface. As a result of the occurrence of plastic deformation brought on by friction and high temperature, which resulted in a decrease in the hardness values, the presence of cracks, and the beginnings of a separation process, the bond between the base and the paint layer weakens when the percentage of addition to the rest of the mixtures is reduced. Regarding the models that contain an additional proportion (25%) of all combinations, there is a process of paint layer separation, the existence of cracks, and a considerable reduction in wear rate. The bond between the base and the paint layer weakens when the percentage of addition to the other mixtures is decreased because of the occurrence of plastic deformation caused by friction and high temperature, which resulted in a decrease in the hardness values, the presence of cracks, and the beginnings of a separation process. There is a process of paint layer separation, the presence of cracks, and a noticeably lower wear rate for the samples that have an additional portion (25%) of all combinations. According to the results for wear rate, hardness is the most significant factor influencing it. Increasing hardness decreases wear rate and enhances adhesion strength, according to the research by E. Rabinowicz,[19] who looked at how wear rate changed as a function of hardness.

The effect of percentage additives materials on the coating porosity

The findings of the porosity measurements revealed that the coating material appeared to have pores in varying percentages depending on the three sedimentation rates that were permitted for use in our research (Ni-WC, Ni-B_4C, and Ni-WC-B_4C). According

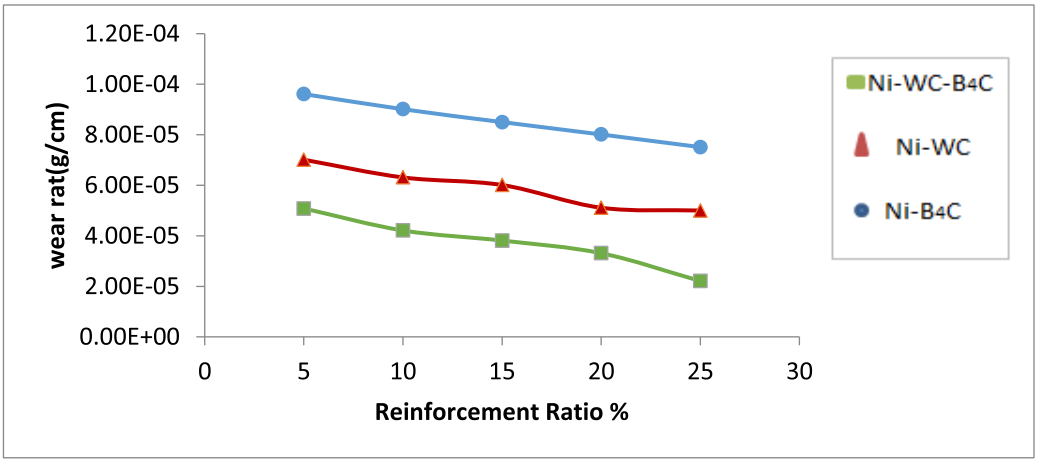

Fig. 7. The correlation between backing materials and coating wear rate.

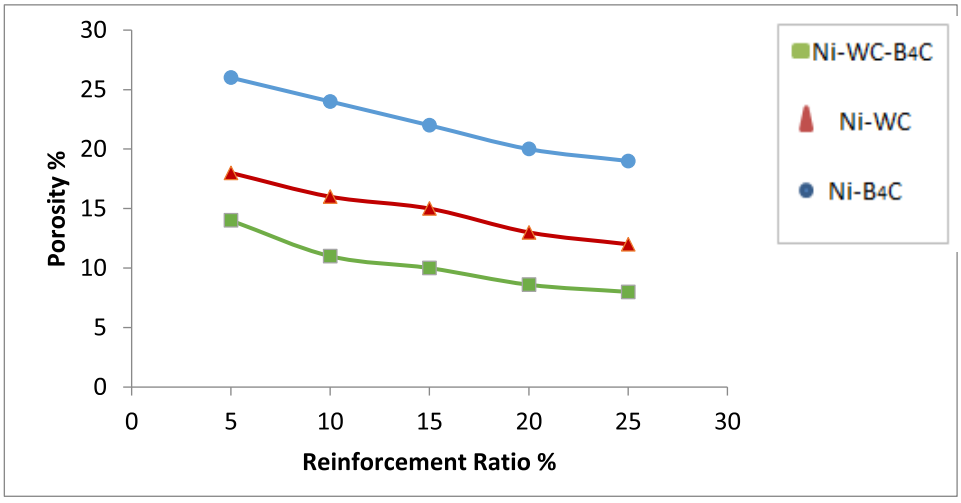

Fig. 8. Show the connection between the porosity and the additive materials.

to Fig. 8, observation the percentage of pores ranged between 8 % and 19 % for the 25 % (Ni-WC-B_4C), whereas the percentage for the 25 % (Ni-WC) was equal to 12%. According to Fig. 8, all of the employed sedimentation ratios have very large porosities when the cementing ratios are low. As the cementing ratios rise, the porosity gradually decreases until it reaches its lowest level at the mixing ratio (25%) (Ni-WC-B_4C). Due to the speed and temperature of the molten particles being higher in the center of the spraying than at the borders, the molten particles do not distribute evenly throughout the surface of the base 131, and as a result, they do not become molten. This change in porosity is the result of the cermet coating layers forming bonding areas between them as a result of sintering and atom diffusion occurring due to the movement of atoms between them, and their attempt to seal the pores during heat treatment.[20]

Scanning electron microscope

Thermal spray coating of flame was used to examine the surface topography of the samples sprayed using the thermal spray technique. The scanning electron microscope with a depth of 10 μm and magnification is shown in Fig. 9 (5KX). Before the heat sintering process, it provides samples for the scanning electron microscope. The scanning electron microscope is shown in Fig. 10. After thermal sintering at 1050˚C for an hour and a half with three distinct combinations that included (Ni-WC-B_4C) 25%, (Ni-B_4C) 25%, and (Ni-WC) 25%, the samples were examined under (5KX) magnification and at (10 μm depth). Although the image (Ni-WC) depicts the coating process' success, the sample still had random atom distribution throughout its surface, as well as cracks with distinct features. However, after carrying out the thermal sintering process, it was found that

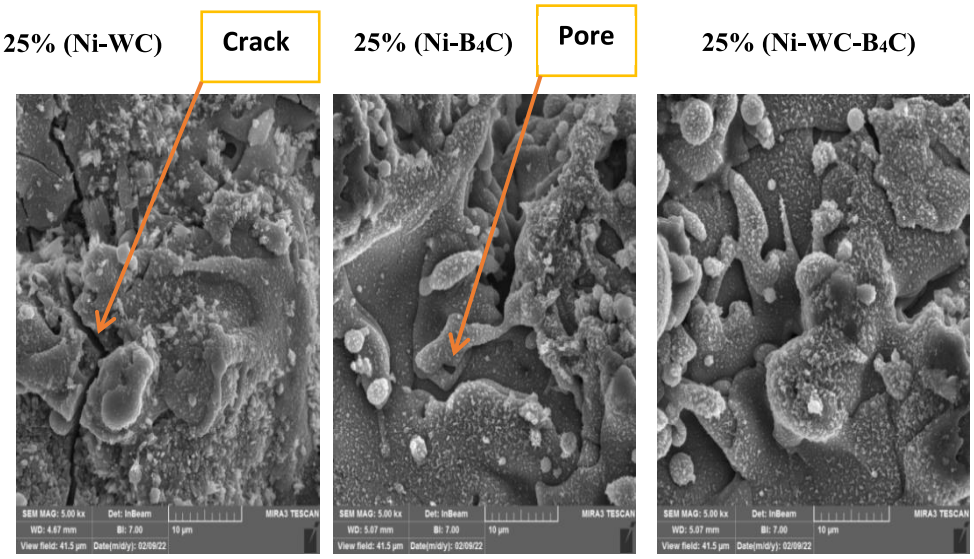

Fig. 9. Scanning electron microscopy (SEM) images of the three mixtures before the thermal sintering process at 1050°C.

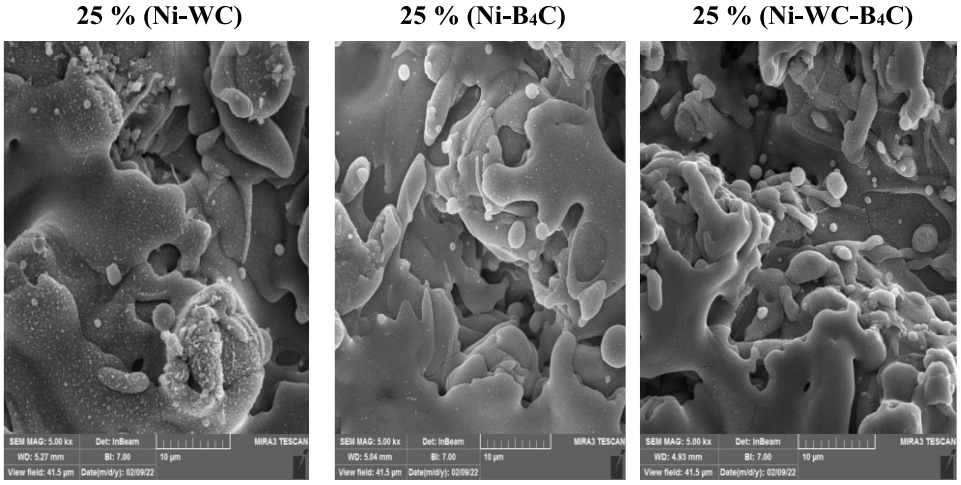

Fig. 10. Scanning electron microscopy (SEM) images of the three mixtures after the thermal sintering process at 1050°C.

the sample has clearly improved and had acceptable homogeneity. Regarding the picture (Ni-B_4C), it was observed the reinforcement material is obviously dispersed throughout the nickel, as evidenced by the randomness of the surface and the existence of pores through the surface, which adversely affects the physical and mechanical properties of the samples. However, after the thermal sintering process, the surface and structural characteristics of the prepared samples improve.[21,22] The reinforcing rate for the image (Ni-WC-B_4C) is 25%. It was observed that a very uniform and clean surface is produced, and each of the base and support materials has crystalline interweaving. The topography of the surface has a significant bearing on understanding the composition of the external coating and how the crystalline granules of the three elements grow, as the size and shape of the granules have a significant bearing on the results obtained in hardness, porosity, and adhesion strength. After conducting the thermal sintering process, it was noticed notice that the three overlays are distributed in all parts of the surface. Due to these factors, dependence is placed When used to cover turbine blades or other items that are subjected to high temperatures, cermet coatings can be highly useful.[23,24]

Conclusion

It was possible to apply the coating method by thermal spraying with a flame to paint each of the three metals—nickel, tungsten carbide, and boron

carbide—in an integrated manner and to obtain encouraging physical properties that allow it to paint turbine blades that have external cracks and pores. This is a clear and significant conclusion. When a type C mixture of 50% Ni, 25% WC, and 25% B_4C was sprayed at a distance of 15 cm, an angle of 90°, and a temperature of 1050°C, the best results were obtained, the hardness was 240 Hv, and the adhesion strength was 39MPa. The best coating thickness for both adhesion and hardness is (1.5 mm), while the least amount of wear is 2.21×10^{-5}g/cm and porosity has dropped to 8%. In particular, following the heat sintering procedure, the results of the scanning electron microscope showed good homogeneity and mechanical crosslinking at the same ratio mentioned.

Acknowledgment

Thanks to everyone who contributed to the completion of this work

Author's declaration

- Conflicts of Interest: None.
- We hereby confirm that all the Figures and Tables in the manuscript are ours. Besides, the Figures and images, which are not ours, have been given the permission for re-publication attached with the manuscript.
- No animal studies are present in the manuscript.
- No human studies are present in the manuscript.
- Ethical Clearance: The project was approved by the local ethical committee at University of Tikrit.

Author's contribution statement

This work was carried out in collaboration between M. M. H., S. Y. D., and A. SH. M. Contributed to the design and implementation of the research, to the analysis of the results and the writing of the manuscript.

References

1. Meghwal A, Anupam A, Murty BS, Berndt CC, Kottada RS, Ang ASM, Thermal spray high-entropy alloy coatings: A review. J Therm Spray Technol. 2020,29:857–893, https://dio.org/10.1007/s11666-020-01047-0.
2. Bhadauria A, Rana D, Balani K, Classification of thermal spray techniques. In Fundamentals of Thermal Spraying, 2023, 1st Edition. 47–77. CRC Press, https://doi.org/10.1201/9781003321965
3. Hou QY, Huang HQ, Zhou DH, Wang P, Xie Q, Huang ZY, Influence of NbC-doping on the microstructure and thermomechanical properties of tungsten coating fabricated by supersonic atmospheric plasma spraying. Surf Coat Technol. 2020;394:125823, https://doi.org/10.1016/j.surfcoat.2020.125823.
4. Wang G, Dai Y, Yang H, Xiong Q, Wang K, Zhou J, *et al*, A review of recent advances in biomass pyrolysis. Energy Fuels. 2020;34(12):15557–15578, https://doi.org/10.1021/acs.energyfuels.0c03107.
5. Prashar G, Vasudev H, A review on the influence of process parameters and heat treatment on the corrosion performance of Ni-based thermal spray coatings. Surf Rev Lett. 2022;29(01):2230001, https://doi.org/10.1142/S0218625$\times$22300015.
6. Darweesh SY, Ali AM, Khodair ZT, Majeed ZN, The effect of some physical and mechanical properties of cermet coating on petroleum pipes prepared by thermal spray method. J Fail Anal Prev. 2019;19(6):1726–1738, https://dio.org/10.1007/s11668-019-00772-1.
7. Xie LL, Chu JH, Li XJ, Zou DN, Tong LB, Improved corrosion resistance of EP coating on Mg alloy through GO hybridization and silica-based superhydrophobic surface. Diam Relat Mater. 2022;130:109476, https://doi.org/10.1016/j.diamond.2022.109476.
8. Sílvia RC, Lauro CH, Ana H, Davim JP, Development of FEM-based digital twins for machining difficult-to-cut materials: A roadmap for sustainability. J Manuf Process. 2022;75:739–766, https://doi.org/10.1016/j.jmapro.2022.01.027.
9. Ctibor P, Sedlacek J, Musalek R, Tesar T, Lukac F, Structure and electrical properties of yttrium oxide sprayed by plasma torches from powders and suspensions. Ceram Int. 2022;48(6):7464–7474, https://doi.org/10.1016/j.ceramint.2021.11.291
10. Li Y, Liu J, Deng J, He J, Qin Y, Xing Y, *et al*, Fabrication of graphene oxide reinforced plasma sprayed Al2O3 coatings. Ceram Int. 2023;49(2):1667–1677, https://doi.org/10.1016/j.ceramint.2022.09.129.
11. Humeedi SH, Abdulkareem SM, Darweesh SY, (2022). The synthetic and mechanical properties of a silica matrix cermet composite. Journal of Wuhan University of Technology-Mater. Sci. Ed., 37(3):423–428. https://doi.org/10.1016/j.jksues.2024.02.001
12. Khan PA, Thoutam AK, Gopal V, Gurumallesh A, Joshi S, Palaniappan A, *et al.* Influence of graphene nanoplatelets on the performance of axial suspension plasma-sprayed hydroxyapatite coatings. Bioeng. 2022;10(1):44, https://doi.org/10.3390/bioengineering10010044.
13. Amanov A, Berkebile SP, Enhancement of sliding wear and scratch resistance of two thermally sprayed Cr-based coatings by ultrasonic nanocrystal surface modification. Wear. 2023;512:204555, https://doi.org/10.1016/j.wear.2022.204555.
14. Torresani E, Carrillo M, Haines C, Martin D, Olevsky E, Fabrication of powder components with internal channels by spark plasma sintering and additive manufacturing. J Eur Ceram Soc. 2023;43(3):1117–1126, https://doi.org/10.1016/j.jeurceramsoc.2022.11.008.
15. Ariharan S, Hassan R, Balani K, Spraying parameters. In Fundamentals of Thermal Spraying, 2023; pp. 79-96. CRC Press, https://doi.org/10.1201/9781003321965.
16. Karim A S, Majeed Z N, Darweesh S Y. The effect of nanostructured zirconia reinforcement on the mechanical and structural properties of a copper-based system. Mater Sci Forum. 2021;

1039: 297-306. Trans Tech Publications Ltd. https://doi.org/10.4028/www.scientific.net/MSF.1039.297.
17. Sridhar K, Balasubramanian V, Erosion–corrosion-resistant coatings for seawater piping components—A review. A Treatise on Corrosion Science, Engineering and Technology. 2022;591–610, https://dio.org/10.1007/978-981-16-9302-1_30.
18. Medabalimi SR, Ramesh MR, Kadoli R, Developing partially oxidized NiCr coatings using the combined flame spray and plasma spray process for improved wear behavior at high temperature. Wear. 2021;478:203885, https://doi.org/10.1016/j.wear.2021.203885.
19. Schmidt W, Heck P, Gaedigk C, Groche P, Static friction in oil lubricated cold forming processes. Tribol Lett. 2022;70(1):12, https://doi.org/10.1007/s11249-021-01553-4.
20. Wang Q, Sun Q, Zhang MX, Niu WJ, Tang CB, Wang KS, *et al.* The influence of cold and detonation thermal spraying processes on the microstructure and properties of Al-based composite coatings on Mg alloy. Surf Coat Technol. 2018;352:627–633, https://doi.org/10.1016/j.surfcoat.2018.08.045.
21. Khalid A, Abbas M, Zhang Y, Hyland M, Munroe PR, Microstructural study of Ni and Ni-20Cr particles plasma sprayed on stainless steel substrate at 300° C. Appl Surf Sci. 2022;592:153320, https://doi.org/10.1016/j.apsusc.2022.153320.
22. Ma X, Ruggiero P, Bhattacharya R, Senkov ON, Rai AK, Evaluation of new high entropy alloy as thermal sprayed bondcoat in thermal barrier coatings. J Therm Spray Technol. 2021;1–10, https://doi.org/10.1007/s11666-021-01279-8.
23. Hameed MM, Al-Samarai AME, Aadim KA. Synthesis and characterization of gallium oxide nanoparticles using pulsed laser deposition. Iraqi J Sci. 2020;25822589.
24. Ibraheem AM, Allah SMA, Darweesh SY. Enhancement the properties of aluminum by adding boron carbide by the powder method. J Phys : Conf Ser. 2021;1999(1):012074. IOP Publishing. doi:10.1088/1742-6596/1999/1/012074.

تأثير الإضافات المتكررة على الخصائص التركيبية والفيزيائية لمعدن النيكل باستخدام الرش الحراري باللهب

محمد مجيد حميد[1]، صالح يونس درويش[2]، عامر شاكر محمود[3]

[1]وزارة التعليم العالي والبحث العلمي
[2]قسم الفيزياء، كلية العلوم، جامعة تكريت، تكريت، العراق .
[3]قسم الفيزياء، كلية التربية للعلوم الصرفة، جامعة تكريت، تكريت، العراق.

الخلاصة

طريقة الرش الحراري باللهب هي الطريقة التي تم استخدامها لإجراء طلاء يتكون من قاعدة النيكل وإضافات من ثلاث مجموعات (C = Ni-WC-B_4C)، (B = Ni-B_4C) ، و (A = Ni- WC) وبنسب تقوية مختلفة من هذه المجموعات ، تشكل أساس طلاء سيرميت. تم صنع قواعد الرش الحراري عن طريق تقطيع وقطع ريش التوربينات والتي كانت على شكل 1 سم مربع معطلة عن الخدمة. ان زاوية الرش 90° ، مسافة الرش 15cm ، درجة حرارة التلبيد الحراري 1050°C ، ونسبة الخلط من النوع (C=50%Ni-25%WC-25%B4C) للخلطات الثلاثة وكانت في ظروفها القياسية المثالية. أظهرت نتائج المجهر الإلكتروني الماسح تجانسًا وتشابكًا ميكانيكيًا جيدًا تقريبًا وبنفس النسبة أعلاه ، خاصة بعد عملية التلبيد الحراري. تم اكتشاف أن الصلابة (240 Hv) وقوة الالتصاق (39 MPs) وأفضل سماكة طلاء عند كل من الصلابة وقوة الالتصاق (1.5 mm) .تم الملاحظة أيضًا عن أن الخليط (C) ، الذي كان يتمتع بقدرات تركيبية وفيزيائية وميكانيكية فائقة مقارنة بالمجموعات (B) و (A) ، قد أعطي أفضل النتائج.

الكلمات المفتاحية: كربيد البورون ، الطلاء السيرميتي ، سمك الطلاء ، الميكروسكوب الإلكتروني الماسح ، الرش الحراري.